Inorganic Chemistry

Article

pubs.acs.org/IC

Borane-Protected Cyanides as Surrogates of H-Bonded Cyanides in [FeFe]-Hydrogenase Active Site Models

Brian C. Manor, Mark R. Ringenberg, and Thomas B. Rauchfuss*

School of Chemical Sciences, University of Illinois, Urbana, Illinois 61801, United States

Supporting Information

ABSTRACT: Triarylborane Lewis acids bind $[Fe_2(pdt)(CO)_4(CN)_2]^{2-}$ $[\mathbf{1}]^{2-}$ (pdt^{2-} = 1,3-propanedithiolate) and $[Fe_2(adt)(CO)_4(CN)_2]^{2-}$ $[\mathbf{3}]^{2-}$ (adt^{2-} = 1,3-azadithiolate, $HN(CH_2S^-)_2$) to give the 2:1 adducts $[Fe_2(xdt)(CO)_4(CNBAr_3)_2]^{2-}$. Attempts to prepare the 1:1 adducts $[\mathbf{1}(BAr_3)]^{2-}$ (Ar = Ph, C_6F_5) were unsuccessful, but related 1:1 adducts were obtained using the bulky borane $B(C_6F_4\text{-}o\text{-}C_6F_5)_3$ ($BAr^F{}^*{}_3$). By virtue of the N-protection by the borane, salts of $[Fe_2(pdt)(CO)_4(CNBAr_3)_2]^{2-}$ sustain protonation to give hydrides that are stable (in contrast to $[H\mathbf{1}]^-$). The hydrides $[H\mathbf{1}(BAr_3)_2]^-$ are 2.5−5 pK_a units more acidic than the parent $[H\mathbf{1}]^-$. The adducts $[\mathbf{1}(BAr_3)_2]^{2-}$ oxidize quasi-reversibly around −0.3 V versus $Fc^{0/+}$ in contrast to ca. −0.8 V observed for the $[\mathbf{1}]^{2-/-}$ couple. A simplified synthesis of $[\mathbf{1}]^{2-}$, $[\mathbf{3}]^{2-}$, and $[Fe_2(pdt)(CO)_5(CN)]^-$ ($[\mathbf{2}]^-$) was developed, entailing reaction of the diiron hexacarbonyl complexes with KCN in MeCN.

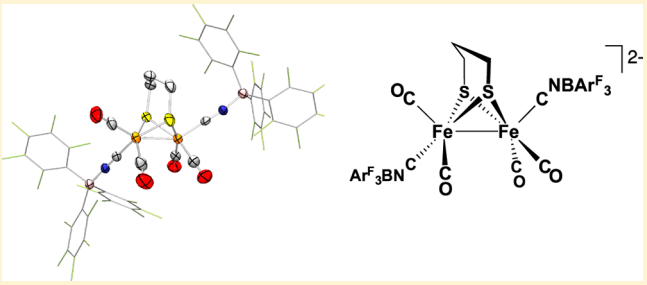

INTRODUCTION

A highlight in the history of bioorganometallic chemistry is the discovery of cyanide ligands as cofactors in the [FeFe] and [NiFe] hydrogenases (H_2ases).[1] The role of cyanide in H_2ases remains underdetermined since few models incorporating this cofactor are available for testing, and those models that do exist exhibit reactions highly complicated by the behavior of the cyanide ligands.[2] Hydrogen bonding between the protein backbone and cyanide is known to anchor the active sites, which are otherwise lightly tethered to the protein.[3] Cyanide is a powerful σ-donor ligand that in part serves to stabilize the ferrous state, as illustrated by the redox inactivity of the $Fe(CN)_2(CO)$ center in the [NiFe] H_2ases.[4] The situation is different in the [FeFe] H_2ases since each Fe center carries one cyanide and at least one of the Fe centers undergoes redox.[5]

In synthetic analogues, cyanide interferes with the two key attributes of functional models: acid/base and redox reactions. Thus, even though salts of $[Fe_2(pdt)(CO)_4(CN)_2]^{2-}$ (pdt^{2-} = 1,3-propanedithiolate), $[\mathbf{1}]^{2-}$, were described in 1999,[6,7] little work has been reported since their initial discovery in part because the products of protonation and oxidation of $[\mathbf{1}]^{2-}$ are unstable. Protonation of $(Et_4N)_2[\mathbf{1}]$ occurs initially at the basic Fe−C*N* followed by formation of the μ-hydrido derivative $Et_4N[(\mu\text{-}H)Fe_2(pdt)(CO)_4(CN)_2]$ ($Et_4N[H\mathbf{1}]$), which exists as two major isomers.[8,9] The salt $Et_4N[H\mathbf{1}]$ is labile, with a half-life of minutes in solution. Both chemical and electrochemical studies indicate that oxidized derivatives of $[\mathbf{1}]^{2-}$ are unstable.[10] As a consequence of the problems associated with cyanide-centered reactions, most functional models feature phosphine ligands as surrogates.[11,12]

Although cyanide is not compatible with many modeling schemes owing to its ambidentate reactivity, nature prevents such problems by encapsulating the active site in globular proteins. The crystal structures of the [FeFe] H_2ases demonstrate the significance of hydrogen bonding to cyanide as observed in the 1.39 Å structure for the CpI enzyme from *Clostridium pasteurianum* (Figure 1).[13] The distal Fe−C*N* is strongly hydrogen-bonded to the ammonium center of Lys358 (N···N distance = 2.74 Å).[14] The lysine group is highly conserved, and this specific hydrogen-bonding interaction has been shown to be critical for activity.[3,15] The proximal cyanide

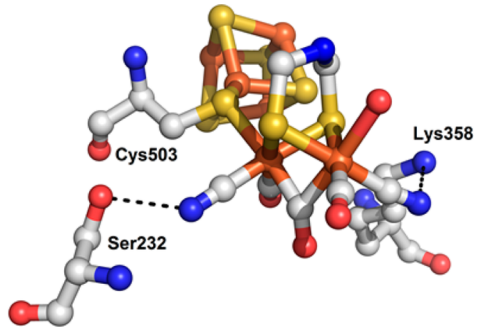

Figure 1. Active site of [FeFe] H_2ase (PDB 3C8Y) depicting hydrogen bonding environment to the cyanide ligands.

Received: February 27, 2014
Published: July 3, 2014

is also weakly hydrogen bonded to Ser232 (N···O distance = 2.92 Å).

The present work is premised on the idea that hydrogen bonding to Fe−C*N* centers can be simulated by FeCN−BR_3 interactions. The ability of triarylboranes to bind to cyanide ligands is well-established as exemplified by *trans*-RuH(CNBPh$_3$)(diphos)$_2$, Ni(diphos)(π-allyl)(CNBPh$_3$), [M(CNBAr$^F_3$)$_4$]$^{2-}$ (M = Ni, Pd; BAr$^F_3$ = B(C$_6$F$_5$)$_3$), and FeCp(CNBAr$^F_3$)(CO)$_2$ (diphos = diphosphine).[16−18] Motivated by interest in frustrated Lewis pairs (FLPs)[19] and the role of boranes in alkene-polymerization,[20] the chemistry of boranes has rapidly developed,[21] as have methods to evaluate their Lewis acidities.[22] Recently, BAr$^F_3$ was used to convert the unreactive species (CO)$_2$(CN)$_2$Fe(pdt)Ni(dxpe) (dxpe = dppe, dcpe) into hydride-containing model catalysts capable of catalytic oxidation of H_2.[23] In parallel with these results, borane Lewis acids were examined with [FeFe]-H_2ase active site models, as described below.

RESULTS

Synthesis of [Fe$_2$(pdt)(CO)$_5$(CN)]$^-$ and [Fe$_2$(xdt)(CO)$_4$(CN)$_2$]$^{2-}$ (xdt = adt, pdt). A new synthesis was developed for cyanide-containing [FeFe]-H_2ase models using KCN as a cyanide source (Scheme 1). Quaternary ammonium salts (R$_4$N$^+$, R = Et, Bu) salts of cyanide had previously been used to generate the same anions.[6,7] The salt K$_2$[**1**] formed in good yields upon treating Fe$_2$(pdt)(CO)$_6$ with an excess of KCN in refluxing MeCN. The salt K$_2$[Fe$_2$(adt)(CO)$_4$(CN)$_2$] (adt^{2-} = 1,3-azadithiolate, HN(CH$_2$S$^-$)$_2$) (K$_2$[**3**]) was prepared analogously, also in good yield. The potassium salts are soluble in MeCN and even dissolve in tetrahydrofuran (THF) and Et$_2$O in the presence of small amounts of MeCN. As we show below, the K$^+$ in these salts usefully modifies the basicity of the Fe−C*N* centers, allowing the synthesis of complexes unattainable as their Et$_4$N$^+$ salts. The monocyanides K[Fe$_2$(pdt)(CO)$_5$(CN)] (K[**2**]) and K[Fe$_2$(adt)(CO)$_5$(CN)] were observed as respective intermediates in the formation of K$_2$[**1**] and K$_2$[**3**]. Using a slight deficiency of KCN, K[**2**] could be prepared in excellent yield from the hexacarbonyl. Like Et$_4$N[**2**], K[**2**] exhibits good solubility in MeCN and THF.

Scheme 1

$$Fe_2(pdt)(CO)_6 + 2\,KCN \rightarrow \underset{K_2[\mathbf{1}]}{K_2[Fe_2(pdt)(CO)_4(CN)_2]} + 2\,CO$$

$$Fe_2(pdt)(CO)_6 + KCN \rightarrow \underset{K[\mathbf{2}]}{K[Fe_2(pdt)(CO)_5(CN)]} + CO$$

$$Fe_2(adt)(CO)_6 + 2\,KCN \rightarrow \underset{K_2[\mathbf{3}]}{K_2[Fe_2(adt)(CO)_4(CN)_2]} + 2\,CO$$

In the IR spectra of K$_2$[**1**] and K$_2$[**3**], the ν_{CO} and ν_{CN} bands occur at slightly higher energy than the analogous Et$_4$N$^+$ compounds (Table 1).[10,24] This shift may be attributed to the coordination of K$^+$ to the cyanide ligands as observed previously for K[CpFe(CO)(CN)$_2$].[25] The salt K$_2$[**1**] was found to undergo anion exchange with PPNCl and Et$_4$NCl in MeCN, shifting ν_{CN} and ν_{CO} to lower energy, matching the previously reported IR spectrum.[6,26]

2:1 Borane Adducts of [Fe$_2$(pdt)(CO)$_4$(CN)$_2$]$^{2-}$. The Lewis acid BAr$^F_3$ binds to the nitrogen centers of [**1**]$^{2-}$ to give stable adducts (eq 1).

Table 1. IR Bands in the ν_{CN} and ν_{CO} Regions for Et$_4$N$^+$ and K$^+$ Salts of [1]$^{2-}$, [2]$^-$, and [3]$^{2-}$

compound	ν_{CN} (cm^{-1})	ν_{CO} (cm^{-1})
(Et$_4$N)$_2$[**1**]^a	2075	1964, 1924, 1885
K$_2$[**1**]^a	2077	1967, 1928, 1890
Et$_4$N[**2**]^b	2094	2029, 1974, 1955, 1941, 1917
K[**2**]^a	2092	2031, 1976, 1956, 1946, 1916
(Et$_4$N)$_2$[**3**]^a	2075	1969, 1925, 1892
K$_2$[**3**]^a	2078	1969, 1929, 1893

^{a}MeCN solution. ^{b}THF solution, ref 10.

$$\underset{[\mathbf{1}]^{2-}}{[Fe_2(pdt)(CO)_4(CN)_2]^{2-}} + 2BAr_3 \rightarrow \underset{[\mathbf{1}(BAr_3)_2]^{2-}}{[Fe_2(pdt)(CO)_4(CNE} \quad (1)$$

In addition to BAr$^F_3$, the weaker Lewis acids BPh$_3$ and B(2,4,6-C$_6$H$_2$F$_3$)$_3$ (BAr$^{F\#}_3$) also formed related adducts. Treatment of a CH_2Cl_2 solution of (Et$_4$N)$_2$[**1**] with 2 equiv of these Lewis acids resulted in lightening of the solution color from red to orange. Upon binding of the borane, IR bands in the ν_{CO} and ν_{CN} regions shift to higher frequencies (Table 2). On the basis of the ν_{CO} bands for the adducts, the relative Lewis acidities of the boranes were BAr$^F_3$ > BAr$^{F\#}_3$ > BPh$_3$, as established by Child's methods,[22,27,28] computational methods, and other studies.[29,30] The coordination of Lewis acids greatly increased the solubility of the complexes. Whereas the uncapped compound (Et$_4$N)$_2$[**1**] is soluble in MeCN and CH_2Cl_2, the adducts [**1**(BAr$_3$)$_2$]$^{2-}$ are soluble in THF and, in the case of [**1**(BAr$^F_3$)$_2$]$^{2-}$, even in Et$_2$O.

Table 2. IR Bands for (Et$_4$N)$_2$[1**(BAr$_3$)$_2$] and Related Complexes in CH_2Cl_2 Solution**

compound	ν_{CN} (cm^{-1})	ν_{CO} (cm^{-1})
(Et$_4$N)$_2$[**1**]	2075	1964, 1924, 1885
(Et$_4$N)$_2$[**1**(BPh$_3$)$_2$]	2137	1984, 1946, 1911
(Et$_4$N)$_2$[**3**(BPh$_3$)$_2$]	2136	1986, 1949, 1914
(Et$_4$N)$_2$[**1**(BAr$^{F\#}_3$)$_2$]	2147	1986, 1947, 1915
(Et$_4$N)$_2$[**1**(BAr$^F_3$)$_2$]	2136	1990, 1954, 1922
Fe$_2$(pdt)(CO)$_4$(PMe$_3$)$_2$[31]		1979, 1942, 1889
Fe$_2$(pdt)(CO)$_4$(CN^{t}Bu)$_2$[32]	2145	1997, 1972, 1933

Rapid turnstile rotation of Fe(CO)$_2$(CNBAr$_3$) centers was indicated by observation of a single BAr$_3$ environment in the ^{1}H NMR spectra of [**1**(BPh$_3$)$_2$]$^{2-}$ and [**1**(BAr$^{F\#}_3$)$_2$]$^{2-}$. Similarly, the ^{19}F NMR spectra of [**1**(BAr$^{F\#}_3$)$_2$]$^{2-}$ and [**1**(BAr$^F_3$)$_2$]$^{2-}$ showed only a single averaged environment. The Fe−CNBAr$_3$ linkage was confirmed by ^{11}B NMR spectra. The ^{11}B NMR spectrum of [**1**(BAr$^F_3$)$_2$]$^{2-}$ adducts feature a broadened signal at δ −14. For the alternative linkage isomer Fe−NC−BAr$_3$, a sharp signal is expected near δ −20.[18] Similarly, the ^{11}B NMR spectrum of [**1**(BPh$_3$)$_2$]$^{2-}$ exhibits a broad signal at δ −4.5, consistent with a M−CNBPh$_3^-$ linkage.[17] The ^{11}B NMR spectrum of [**1**(BAr$^{F\#}_3$)$_2$]$^{2-}$ exhibits a broad signal at δ −15.

The structure of (Et$_4$N)$_2$[**1**(BAr$^F_3$)$_2$] was confirmed by X-ray crystallography (Figure 2). Reassuring for our modeling efforts, no obvious structural differences exist between (Et$_4$N)$_2$[**1**(BAr$^F_3$)$_2$] and the previously reported structure of (Et$_4$N)$_2$[**1**][10] (Supporting Information, Table S3). For example, the Fe−Fe, C≡N, Fe−CO, and C≡O distances differ by less than 0.02 Å. Slight shortening of the Fe−CN bond

dx.doi.org/10.1021/ic500470z | Inorg. Chem. 2014, 53, 7241−7247

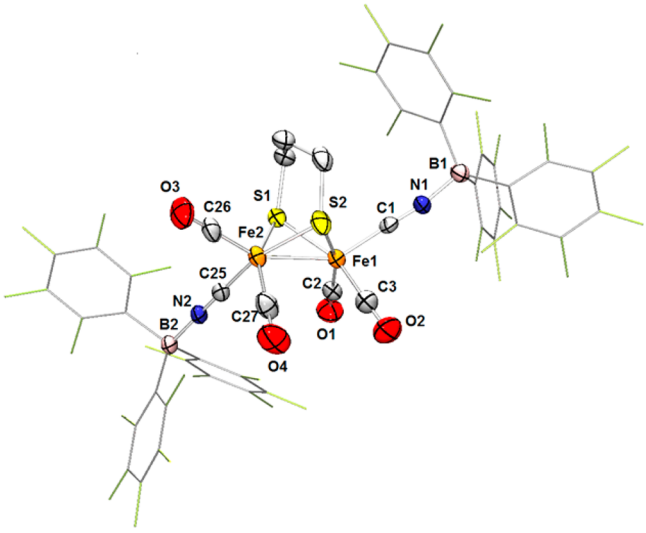

Figure 2. Thermal ellipsoid plot of $[\mathbf{1}(BAr^F{}_3)_2]^{2-}$ at 50% probability and with H atoms omitted for clarity. Pentafluorophenyl groups are deemphasized for clarity.

is observed upon coordination of $BAr^F{}_3$, with the Fe−CN bond 0.06 Å shorter for $(Et_4N)_2[\mathbf{1}(BAr^F{}_3)_2]$ than for $(Et_4N)_2[\mathbf{1}]$.

2:1 Borane Adducts of $[Fe_2(adt)(CO)_4(CN)_2]^{2-}$. Given the basicity of the NH center in $[\mathbf{3}]^{2-}$, adducts of this complex with boranes were anticipated to be more complex than they were for $[\mathbf{1}]^{2-}$. IR measurements indicated that addition of 2 equiv of $BAr^F{}_3$ to $(Et_4N)_2[\mathbf{3}]$ resulted in an unstable complex. The less Lewis-acidic BPh_3 afforded the desired 2:1 adduct $(Et_4N)_2[Fe_2(adt)(CO)_4(CNBPh_3)_2]$, $(Et_4N)_2[\mathbf{3}(BPh_3)_2]$. The IR spectrum of this salt is very similar to that for $(Et_4N)_2[\mathbf{1}(BPh_3)_2]$ (Table 2). Its ^1H NMR spectrum displayed a single BPh_3 environment, consistent with both BPh_3 groups being bound to Fe-CN centers and rapid rotation of the $Fe(CO)_2(CNBPh_3)$ subunits.

1:1 Borane Adducts of $[Fe_2(pdt)(CO)_4(CN)_2]^{2-}$. Attempts were made to generate the 1:1 borane adducts of $[\mathbf{1}]^{2-}$. As indicated by IR spectroscopy, treatment of $(Et_4N)_2[\mathbf{1}]$ with 1 equiv of $BAr^F{}_3$ or BPh_3 gave a mixture of $(Et_4N)_2[\mathbf{1}(BAr_3)_2]$, starting material, and insoluble solids (that do not redissolve in the presence of boranes). In an effort to stabilize 1:1 adducts, the bulky borane $B(C_6F_4\text{-}o\text{-}C_6F_5)_3$ ($BAr^F{}^*{}_3$) was examined. The reaction of $(Et_4N)_2[\mathbf{1}]$ with 1 equiv of $BAr^F{}^*{}_3$ precipitated intractable solids, even when the addition was conducted slowly and on dilute solutions. When 2 equiv of $BAr^F{}^*{}_3$ were added quickly, the 2:1 adduct $(Et_4N)_2[\mathbf{1}(BAr^F{}^*{}_3)_2]$ formed in good yield.

The formation of 1:1 adducts required starting with $K_2[\mathbf{1}]$ instead of the Et_4N^+ salt. Treatment of $K_2[\mathbf{1}]$ with 1 equiv of $BAr^F{}^*{}_3$ gave $K_2[\mathbf{1}(BAr^F{}^*{}_3)]$ (eq 2).

$$K_2[Fe_2(pdt)(CO)_4(CN)_2] + BAr^F{}^*{}_3 \rightarrow K_2[Fe_2(pdt)(CO)_4(CN)(CNBAr^F{}^*{}_3)] \quad (2)$$

The IR spectrum of this adduct shows ν_{CN} bands at disparate energies (2126, 2058 cm^{-1}), consistent with the coordination of $BAr^F{}^*{}_3$ to a single cyanide ligand (see Figure 3).

The salt $K_2[\mathbf{1}(BAr^F{}^*{}_3)_2]$ was produced in good yield. This pale red solid exhibits good solubility in ether and THF, as found for $(Et_4N)_2[\mathbf{1}(BAr^F{}_3)_2]$. The IR spectra of $K_2[\mathbf{1}(BAr^F{}^*{}_3)]$ and $K_2[\mathbf{1}(BAr^F{}^*{}_3)_2]$ were found to vary with

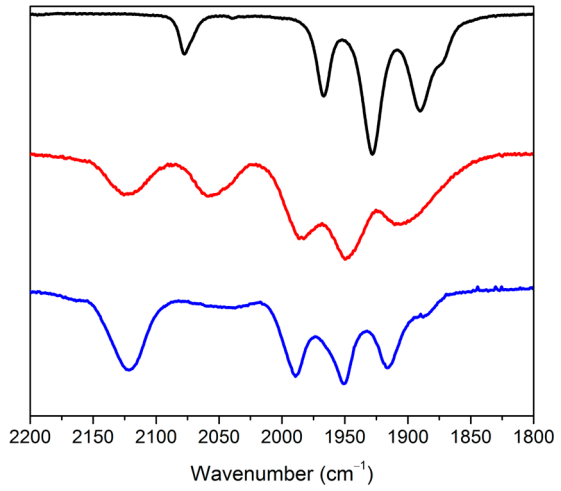

Figure 3. IR spectra of $K_2[\mathbf{1}]$ in MeCN (top), $K_2[\mathbf{1}(BAr^F{}^*{}_3)]$ in CH_2Cl_2 (middle), and $K_2[\mathbf{1}(BAr^F{}^*{}_3)_2]$ in CH_2Cl_2 (bottom).

solvent (CH_2Cl_2 vs MeCN). The solvent effect is reversible. In contrast, the IR spectrum for $(Et_4N)_2[\mathbf{1}(BAr^F{}^*{}_3)_2]$ was unchanged in these solvents (Table 3).

Table 3. IR Bands for $K_2[\mathbf{1}]$ and $(Et_4N)_2[\mathbf{1}]$ and Their $BAr^F{}^*{}_3$ Adducts

compound	solvent	ν_{CN} (cm^{-1})	ν_{CO} (cm^{-1})
$(Et_4N)_2[\mathbf{1}]$	MeCN	2075	1964, 1924, 1885
$K_2[\mathbf{1}]$	MeCN	2077	1967, 1928, 1890
$K_2[\mathbf{1}(BAr^F{}^*{}_3)]$	MeCN	2096, 2081	1990, 1978, 1942, 1931, 1913, 1888
$K_2[\mathbf{1}(BAr^F{}^*{}_3)]$	CH_2Cl_2	2126, 2058	1985, 1950, 1905
$K_2[\mathbf{1}(BAr^F{}^*{}_3)_2]$	MeCN	2098	1991, 1959, 1947, 1932, 1910
$K_2[\mathbf{1}(BAr^F{}^*{}_3)_2]$	CH_2Cl_2	2119	1989, 1951, 1916
$(Et_4N)_2[\mathbf{1}(BAr^F{}^*{}_3)_2]$	MeCN	2098	1991, 1932
$(Et_4N)_2[\mathbf{1}(BAr^F{}^*{}_3)_2]$	CH_2Cl_2	2100	1990, 1928

Hydride Derivatives $[(\mu\text{-H})Fe_2(xdt)(CO)_4(CNBAr_3)_2]^-$ (xdt = adt, pdt). In contrast to the complications reported for the protonation of $[\mathbf{1}]^{2-}$,[9] protonation of the borane adducts $[\mathbf{1}(BAr_3)_2]^{2-}$ proceeded straightforwardly (eq 3).

$$[Fe_2(pdt)(CO)_4(CNBAr_3)_2]^{2-} + H^+ \rightarrow [(\mu\text{-H})Fe_2(pdt)(CO)_4(CNBAr_3)_2]^- \quad (3)$$

Exploiting their distinctive solubility, the borane complexes $(Et_4N)_2[\mathbf{1}(BAr_3)_2]$ were protonated as an ether or THF solution with excess $HCl{\cdot}Et_2O$. Protonation is accompanied by a lightening in the solution color and precipitation of Et_4NCl. Protonation causes a shift of both ν_{CO} and ν_{CN} to higher energies, consistent with oxidation of the diiron centers (Table 4).

The hydrido complexes exhibit characteristic high-field ^1H NMR signals. ^1H NMR spectra of $[H\mathbf{1}(BAr_3)_2]^-$ in CD_2Cl_2 solution display two or three hydride signals, depending on the borane. Ignoring the conformation of the Fe_2pdt center, four isomers are possible for $[H\mathbf{1}(BAr_3)_2]^-$, three of which are symmetrical with equivalent $CNBAr_3^-$ ligands (Figure 4). All four isomers are observed for the $[(\mu\text{-H})Fe_2(pdt)(CO)_4(CN^tBu)_2]^+$ system.[32]

dx.doi.org/10.1021/ic500470z | Inorg. Chem. 2014, 53, 7241−7247

Table 4. IR Bands in ν_{CN} and ν_{CO} Regions for $Et_4N[H1(BAr_3)_2]$ and Related Complexes

compound	solvent	ν_{CN} (cm^{-1})	ν_{CO} (cm^{-1})
$Et_4N[H1]$	MeCN	2118, 2112	2045, 2024, 1985
$Et_4N[H1(BPh_3)_2]$	CH_2Cl_2	2180	2064, 2043, 2009
$Et_4N[H1(BAr^{F\#}{}_3)_2]$	CH_2Cl_2	2194	2066, 2046, 2012
$Et_4N[H1(BAr^{F}{}_3)_2]$	CH_2Cl_2	2185	2071, 2051, 2022
$[(\mu\text{-H})Fe_2(pdt)(CO)_4(PMe_3)_2]BF_4$[31]	CH_2Cl_2		2029, 1989
$[(\mu\text{-H})Fe_2(pdt)(CO)_4(CN^tBu)_2]BF_4$[32]	CH_2Cl_2	2187	2076, 2060, 2028

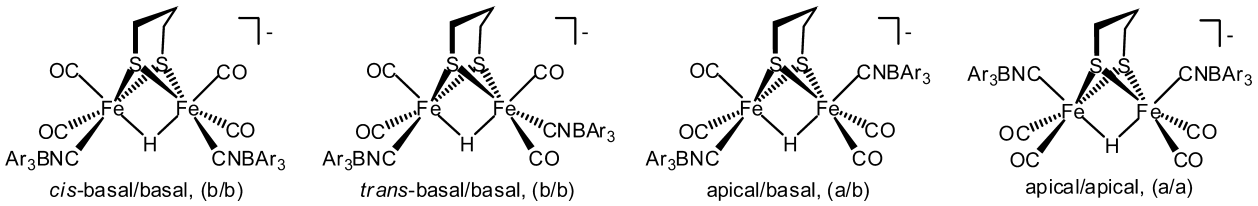

Figure 4. Isomers of $[H1(BAr_3)_2]^-$. Only for the a/b isomer are the $CNBAr_3^-$ ligands nonequivalent.

Freshly generated solutions of $[H1(BAr^F{}_3)_2]^-$ consist of three isomeric hydrides, indicated by ^1H NMR signals at δ −13.7, −16.4, and −19.0 in a ratio of 1:11:5. Over the course of 2 d, the isomer ratio shifted to 1:36:32. The structures of these isomers can be partially inferred from the ^{19}F NMR spectra, since the *p*-F signals are well-resolved. On the basis of these data, the ^1H NMR signal at δ −16, which corresponds to the kinetically favored species, is assigned to the unsymmetrical apical/basal (a/b) isomer. The other two hydride signals arise from symmetrical complexes (single ^{19}F NMR signals), probably the b/b and a/a isomers.

The ^1H NMR spectrum of $[H1(BAr^{F\#}{}_3)_2]^-$ consisted of only two high-field signals, at δ −16.4 and −19.2, in a 3:1 ratio. After equilibration over the course of 3 d, this ratio shifted to 1:1.5. In the ^{19}F NMR spectrum of $[H1(BAr^{F\#}{}_3)_2]^-$, the ratio of the *o*-F and *p*-F signals compared to the ratio of the hydride signals are consistent with one symmetric and one asymmetric isomer (Supporting Information). The species with the ^1H NMR signal at δ −16.4 is assigned to the a/b isomer on the basis of the relative intensities of ^1H and ^{19}F NMR signals.

Freshly generated solutions of $[H1(BPh_3)_2]^-$ consisted of three isomers, indicated by ^1H NMR signals at δ −13.3, −16.1, and −19.2 in a ratio of 1.6:4.3:1. This mixture isomerizes over the course of 2 d to a 1:11:11 ratio. The ^1H NMR spectrum of $[H1(BPh_3)_2]^-$ features four signals assigned to the 2,6-protons on BPh_3, the ratio of which are consistent with two symmetric isomers and one asymmetric isomer. On the basis of the integrations of the hydride signals and *ortho*-aryl signals of $[H1(BPh_3)_2]^-$, the high-field signal at δ −16.14 could be assigned as the a/b isomer. The ^1H NMR signals for the symmetrical isomers of $[H1(BAr_3)_2]^-$ are assigned in analogy to the assignments for $[(\mu\text{-H})Fe_2(pdt)(CO)_4(CN^tBu)_2]^+$:[32] The most downfield hydride signal (δ −13.5) is assigned to one of the b/b isomers, presumably trans for electrostatic reasons, and the most upfield hydride signal (δ −19.0) is assigned to the a/a isomer.

The boranes noticeably affect the basicity of the diiron unit. The pK_a^{MeCN} of $[H1]^-$ is estimated to be 16 as it is fully deprotonated by 1 equiv of benzylamine (pK_a^{MeCN} = 16.91).[33] Protonation of $[1]^{2-}$ to give $[H1]^-$ occurs with one equiv 2,4,6-trimethylpyridinium (pKa^{MeCN} = 14.98).[33] As observed with $[H1]^-$, both $[H1(BAr^F{}_3)_2]^-$ and $[H1(BAr^{F\#}{}_3)_2]^-$ can also be reversibly deprotonated. By ^{19}F NMR spectroscopy using anilinium (pK_a^{MeCN} = 10.62) as the acid,[33] the pK_a^{MeCN} of $[H1(BAr^F{}_3)_2]^-$ was calculated to be 10.8 ± 0.2. Examination of mixtures of $[1(BAr^{F\#}{}_3)_2]^{2-}$ and pyridinium (pK_a^{MeCN} = 12.53)[33] gave a pK_a^{MeCN} of 13.5 ± 0.1. Deprotonation of $[H1(BPh_3)_2]^-$ with pyridine did not cleanly reform $[1(BPh_3)_2]^{2-}$, probably because the adducts of this less-acidic borane are labile. The values for ν_{CO} are similar for $[H1(BAr^{F\#}{}_3)_2]^-$ and $[H1(BPh_3)_2]^-$, suggesting that their pK_a values are probably comparable. The hydridic nature of $[H1(BAr^F{}_3)_2]^-$ was investigated by treatment of a CD_2Cl_2 solution of $[H1(BAr^F{}_3)_2]^-$ with Me_3NHBAr^{F24}. ^1H NMR analysis failed to indicate any interaction.

The presence of adt^{2-} in [FeFe]-H_2ase models has been shown to greatly affect the protonation pathway. The protonation of $(Et_4N)_2[3]$ has been previously reported as occurring at the amine, forming $[Fe_2(Hadt)(CO)_4(CN)_2]^-$, $[\alpha\text{-}H3]^-$, followed by slow proton transfer over days to form the unstable bridging hydride $[(\mu\text{-H})Fe_2(adt)(CO)_4(CN)_2]^-$, $[H3]^-$.[34] Unlike the straightforward protonation of $[1(BAr_3)_2]^{2-}$, protonation of $[3(BPh_3)_2]^{2-}$ proved complicated and sensitive to solvent. Using $H(Et_2O)_2B(Ar^{F6})_4$ protonation in MeCN solution resulted in N-protonation ($\Delta\nu_{CN} \approx 10$ cm^{-1}, $\Delta\nu_{CO} \approx 20$ cm^{-1}), whereas protonation in a CH_2Cl_2 solution produced some bridging hydrides (δ −15.3 and δ −18.4) (Ar^{F6} = C_6H_3-3,5-$(CF_3)_2$, Supporting Information).

Electrochemistry of $[Fe_2(pdt)(CO)_4(CNBAr_3)_2]^{2-}$ and $[(\mu\text{-H})Fe_2(pdt)(CO)_4(CNBAr_3)_2]^-$. According to its cyclic voltammogram, a freshly prepared CH_2Cl_2 solution of $(Et_4N)_2[1]$ irreversibly oxidizes at −0.79 V (Figure 5, all potentials vs $Fc^{0/+}$). The process is accompanied by the appearance of a deposit on the working electrode. In contrast, $(Et_4N)_2[1(BAr_3)_2]$ was found to oxidize quasi-reversibly without fouling the electrodes. The oxidation potentials vary between −0.23 and −0.36 V depending on the Lewis acid (Table 5).

The redox properties of $Et_4N[H1]$ have not been evaluated because of the compound's instability. Borane-capping allowed for the observation of a quasi-reversible reduction for $Et_4N[H1(BAr^F{}_3)_2]$ at −1.65 V vs $Fc^{0/+}$. The potentials of the $[1(BAr_3)_2]^{2-/-}$ and $[H1(BAr_3)_2]^{-/2-}$ couples correlated with the Lewis acidity of the borane (Table 5). Reduction of $[H1(BPh_3)_2]^-$ and $[H1(BAr^{F\#}{}_3)_2]^-$ occurred near −1.74 V; however, reversibility was only observed at scan rates above 0.5 V/s. Interestingly, BPh_3 and $BAr^{F\#}{}_3$ had similar effects on the

dx.doi.org/10.1021/ic500470z | Inorg. Chem. 2014, 53, 7241−7247

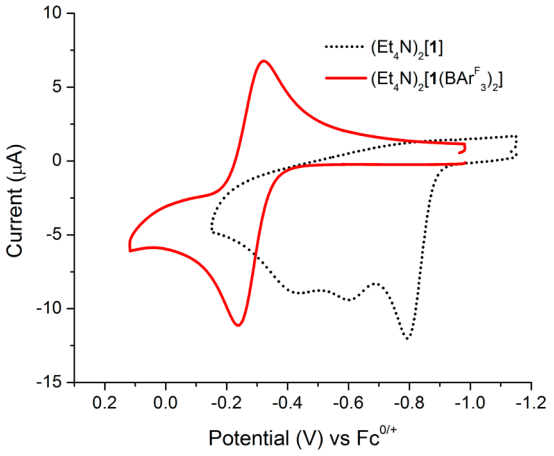

Figure 5. Cyclic voltammograms of $(Et_4N)_2[\mathbf{1}]$ and $(Et_4N)_2[\mathbf{1}(BAr^F{}_3)_2]$ (1 mM solutions in CH_2Cl_2) with 100 mM Bu_4NPF_6 as electrolyte recorded at 0.1 V/s.

redox potentials even though their Lewis acidities are quite different.[28,29,35]

DISCUSSION

A new synthesis of $[\mathbf{1}]^{2-}$ and $[\mathbf{3}]^{2-}$ was developed involving the use of KCN. The method offers advantages over the traditional route: not only is KCN cheaper and safer to use than Et_4NCN, it is commercially available in isotopically labeled forms. Once isolated, $K_2[\mathbf{1}]$ undergoes anion exchange to afford the corresponding Et_4N^+ and PPN^+ salts. In contrast to the use of Et_4NCN, substitution using KCN proceeds via the readily isolated intermediate $K[Fe_2(xdt)(CO)_5(CN)]$.

The coordination of the boranes to $[\mathbf{1}]^{2-}$ and $[\mathbf{3}]^{2-}$ suppresses reactions at the Fe−C*N* sites, which complicated previous studies on the protonation and redox of these very appealing models. Capping the Fe−C*N* sites with boranes allowed for straightforward protonation of $[\mathbf{1}(BAr_3)_2]^{2-}$ to give the μ-hydrido derivatives $[H\mathbf{1}(BAr_3)_2]^-$. Unlike $[H\mathbf{1}]^-$, $[H\mathbf{1}(BAr_3)_2]^-$ was readily isolated and handled. In solution, $[H\mathbf{1}(BAr_3)_2]^-$ exists as a mixture of isomers, the distribution of which is similar for $[(\mu\text{-}H)Fe_2(pdt)(CO)_4(CN^tBu)_2]^+$.[32]

Dihydrogen bonds between a metal hydrides and a protic group is a key interaction in the evolution and oxidation of hydrogen by H_2ases. "Hydridic hydrides" are expected to form dihydrogen bonds with acids.[36] Indeed, crystallographic study of the [FeFe]-H_2ase model $[HFe_2(Hadt)(CO)_2(dppv)_2]^{2+}$, which contains both an N-protonated adt and terminal iron hydride, reveals a short NH···HFe distance of 1.8 Å (dppv = cis-$C_2H_2(PPh_2)_2$).[12] Similarly, NMR measurements indicate intermolecular dihydrogen bonding between $[(CO)(CNBAr^F{}_3)_2Fe(H)(pdt)Ni(dppe)]^-$ and Me_3NH^+.[23] In contrast, we show in this work that the bridging hydride in [FeFe]-H_2ase models do not engage in intramolecular hydrogen bonding.[37] Underscoring the nonhydridic nature of $Fe^{II}(\mu\text{-}H)Fe^{II}$ species, we observed no interaction between $[H\mathbf{1}(BAr_3)_2]^-$ and Me_3NH^+, despite an electrostatic driving force.

The strengths of the hydrogen bonds from the protein to the two CN^- cofactors differ, as reflected by the distances between hydrogen-bonded heteroatoms. The Fe^{distal}−C*N*···N (lysine ε-ammonium) distance is 2.74 Å, whereas the $Fe^{proximal}$−C*N*···O (serine hydroxyl) distance is 2.92 Å.[13] To simulate the disparate nature of these two hydrogen-bonding interactions, attempts were made to bind 1 equiv of a Lewis acid to $[\mathbf{1}]^{2-}$. The reaction of 1 equiv of $BAr^F{}_3$ and $BAr^F{}^*{}_3$ with $(Et_4N)_2[\mathbf{1}]$ gave intractable products. The targeted asymmetrically protected dicyanide complex was obtained by combining the bulky borane $BAr^F{}^*{}_3$ and $K_2[\mathbf{1}]$. We propose that this adduct is stabilized by binding of K^+ to the uncapped FeC*N* center. This interaction is consistent with the solvent dependence of the IR spectra of $K_2[\mathbf{1}(BAr^F{}^*{}_3)]$ and $K_2[\mathbf{1}(BAr^F{}^*{}_3)_2]$. In CH_2Cl_2 solutions, $BAr^F{}^*{}_3$ coordinates strongly to Fe−C*N*, whereas in MeCN solutions K^+ appears to compete with $BAr^F{}^*{}_3$ for coordination to Fe−C*N*. The IR spectrum of $(Et_4N)_2[\mathbf{1}(BAr^F{}^*{}_3)_2]$ was found not to vary with solvent.

In terms of ligand properties, how does $CNBAr^F{}_3^-$ compare with related ligands? The answer depends on the method of measurement. Using the criterion of ν_{CO}, $CNBAr_3^-$ is less basic than PMe_3.[31] Similar ranking is indicated when comparing the pK_a^{MeCN} of the corresponding hydrido complexes.[38] On the other hand, in terms of redox properties, the $[H\mathbf{1}(BAr_3)_2]^{2-/-}$ couple (ca. −1.7 V vs $Fc^{0/+}$) is far more cathodic than the couple $[HFe_2(pdt)(CO)_4(PMe_3)_2]^{+/0}$ (−1.39 V).[39]

Now that adt^{2-} has been established as the dithiolate cofactor,[40] the question remains: what steps are required to convert $[Fe_2(adt)(CO)_4(CN)_2]^{2-}$ and $[(\mu\text{-}H)Fe_2(adt)(CO)_4(CN)_2]^-$ into functioning catalysts? Previously the barrier to this activation was the interfering reactivity of the cyanide ligands, which are both bases and potentially bridging ligands. This distracting behavior has been addressed with the introduction of the borane protecting groups, yet the diferrous hydride remains bridging. One obvious gap is the absence of the 4Fe−4S cluster−ligand on the proximal Fe center. Beyond that omission, the rotated structure may require a more protein-like environment, especially a hydrogen-bonding interaction directed at a basal cyanide on the distal Fe.[3,41]

EXPERIMENTAL SECTION

Materials and Methods. Standard Schlenk or glovebox techniques were used. Solvents used for syntheses were high-performance liquid chromatography grade, further purified by using an alumina filtration system (Glass Contour Co., Irvine, CA), and were deoxygenated prior to use. NMR solvents were purchased from Cambridge Isotope Laboratories, dried with CaH_2, and stored under nitrogen over activated molecular sieves. The preparations of

Table 5. Redox Potentials (V) and Current Ratios of Adducts of $[\mathbf{1}(BAr_3)_2]^{2-}$ and $[H\mathbf{1}(BAr_3)_2]^-$ in CH_2Cl_2 vs $Fc^{0/+}$ (Scan Rate ν = 0.1 V/s)

BAr_3	$E_{1/2}$ $[\mathbf{1}(BAr_3)_2]^{2-/-}$	i_{pa}/i_{pc}	$E_{1/2}$ $[H\mathbf{1}(BAr_3)_2]^{-/2-}$	i_{pc}/i_{pa}	$E_{1/2}[H\mathbf{1}(BAr_3)_2]^{-/0}$	i_{pa}/i_{pc}
none	−0.79	irrev.				
BPh_3	−0.36	0.16	−1.72	irrev. (0.20)[a]		
$BAr^{F\#}{}_3$	−0.34	0.69	−1.76	0.21 (0.44)[a]	1.11	0.76
$BAr^F{}_3$	−0.23	0.82	−1.65	0.28 (0.51)[a]	1.24	0.57

[a] ν = 1.0 V/s.

dx.doi.org/10.1021/ic500470z | Inorg. Chem. 2014, 53, 7241−7247

$(Et_4N)_2$[**1**] and $(Et_4N)_2$[**3**] are described elsewhere.[24,42] $BAr^F{}_3$ was purchased from Boulder Scientific and twice sublimed under vacuum at 90 °C prior to use. BPh_3 was prepared by pyrolysis of $HNMe_3BPh_4$.[43] The preparations of $BAr^F{}^*{}_3$ and $BAr^{F\#}{}_3$ have been reported.[30,44] IR spectra were recorded using a PerkinElmer Spectrum 100 FT-IR instrument using a CaF_2 solution cell. These data are reported in cm^{-1}. Elemental analyses were conducted at the University of Illinois Microanalysis Laboratory. Cyclic voltammetry was performed under nitrogen at room temperature using a CHI 630D potentiostat with glassy carbon working electrode, Pt wire counter electrode, pseudoreference electrode Ag wire, and with ferrocene as an internal standard. NMR spectra were recorded on a Varian Mercury 500 MHz spectrometer, and the ^1H NMR chemical shifts were referenced to the residual protons of deuterated solvents. ^{11}B (recorded on a Varian 400 MHz instrument) and ^{19}F NMR spectra were referenced to external standards of $BF_3{\cdot}Et_2O$ and 1% $CFCl_3$ in $CDCl_3$, respectively.

*$K_2[Fe_2(pdt)(CO)_4(CN)_2]$, K_2[**1**].* A Schlenk flask was charged with $Fe_2(pdt)(CO)_6$ (1.0 g, 2.6 mmol), KCN (0.51 g, 7.8 mmol), and MeCN (100 mL). The mixture was heated at reflux for 28 h, with monitoring by IR spectroscopy. The mixture was filtered through Celite, and the filtrate was evaporated under vacuum. The resulting solid was washed with Et_2O (50 mL) and hexanes (50 mL) and then dried under vacuum. Yield: 0.91 g (76%). Anal. Calcd for $C_9H_6Fe_2K_2N_2O_4S_2{\cdot}0.33CH_3CN$ (found): C, 24.49 (24.35); H, 1.49 (1.64); N, 6.81 (6.88). IR (MeCN): 2077, 1967, 1928, 1890.

*$K[Fe_2(pdt)(CO)_5(CN)]$, K[**2**].* A two-necked Schlenk flask was charged with $Fe_2(pdt)(CO)_6$ (0.50 g, 1.30 mmol), 0.9 equiv of KCN (0.076 g, 1.17 mmol), and MeCN (50 mL). The mixture was heated at reflux for 6 h, with monitoring by IR spectroscopy. The mixture was filtered through Celite, and the filtrate was dried under vacuum. The resulting oil was extracted into Et_2O, and product was precipitated with pentane. The resulting solid was collected by filtration, washed with pentane (50 mL), and dried under vacuum. Yield: 0.42 g (85%). Anal. Calcd for $C_9H_6Fe_2KNO_5S_2$ (found): C, 25.55 (25.62); H, 1.43 (1.71); N, 3.31 (3.17). IR (MeCN): 2092, 2031, 1976, 1956, 1946, 1916.

*$(Et_4N)_2[Fe_2(pdt)(CO)_4(CNBAr^F{}_3)_2]$, $(Et_4N)_2$[**1**$(BAr^F{}_3)_2$].* A slurry of $(Et_4N)_2$[**1**] (2.40 g, 3.74 mmol) in CH_2Cl_2 (50 mL) was treated with $BAr^F{}_3$ (3.88 g, 7.57 mmol) in CH_2Cl_2 (10 mL). After stirring the reaction solution for 30 min, the solvent was evaporated to yield a red oil, which a red powder upon standing under vacuum. The product was triturated with pentane (3 × 10 mL) and crystallized from CH_2Cl_2 (10 mL) layered with Et_2O (10 mL) and pentane (30 mL). Yield: 5.25 g (99%). Anal. Calcd for $C_{61}B_2Fe_2S_2H_{46}O_4N_4F_{30}$ (found): C, 43.97 (43.50); H, 2.78(3.07); N, 3.36 (3.60). IR (CH_2Cl_2): 2136, 1990, 1954, 1922. ^1H NMR (CD_2Cl_2): δ 3.10 (16 H, m, $(CH_3CH_2)_4N$), 1.73 (4 H, t, $SCH_2CH_2CH_2S$), 1.48 (2 H, m, $SCH_2CH_2CH_2$), 1.23 (24 H, t, $(CH_3CH_2)_4N$). ^{11}B NMR (CD_2Cl_2): δ −14. ^{19}F NMR (CD_2Cl_2): δ −134 (d, *o*-F), −162 (t, *p*-F), −167 (t, *m*-F). Crystals suitable for X-ray diffraction were obtained by the slow diffusion of pentane into a THF solution of $(Et_4N)_2$[**1**$(BAr^F{}_3)_2$] at −30 °C.

*$(Et_4N)_2[Fe_2(pdt)(CO)_4(CNBAr^{F\#}{}_3)_2]$, $(Et_4N)_2$[**1**$(BAr^{F\#}{}_3)_2$].* A solution of $(Et_4N)_2$[**1**] (0.16 g, 0.25 mmol) in CH_2Cl_2 (10 mL) was treated dropwise with a solution of $BAr^{F\#}{}_3$ (0.20 g, 0.50 mmol) in 10 mL of CH_2Cl_2. The solvent was evaporated to yield a red oil, which was extracted into CH_2Cl_2 (5 mL). The extract was layered with pentane (20 mL) and cooled at −30 °C for 2 d, producing a red oil. The filtrate was decanted off, and the oil was triturated with pentane (3 × 10 mL) to produce a red solid. Yield: 0.34 g (95%). Anal. Calcd for $C_{61}H_{58}B_2F_{18}Fe_2N_4O_4S_2$ (found): C, 50.51 (50.82); H, 4.03 (4.04); N, 3.86 (4.15). IR (CH_2Cl_2): 2147, 1986, 1947, 1915. ^1H NMR (CD_2Cl_2): δ 6.41 (12 H, t, *m*-Ar*H*), 3.09 (16H, m, $(CH_3CH_2)_4N$), 1.70 (4 H, t, $SCH_2CH_2CH_2S$), 1.42 (2 H, m, $SCH_2CH_2CH_2$), 1.22 (24 H, t, $(CH_3CH_2)_4N$). ^{11}B NMR (CD_2Cl_2): δ −15. ^{19}F NMR (CD_2Cl_2): δ −99.9 (s, *o*-F), −117.1 (s, *p*-F).

*$K_2[Fe_2(pdt)(CO)_4(CN)(CNBAr^F{}^*{}_3)]$, K_2[**1**$(BAr^F{}^*{}_3)$].* A solution of K_2[**1**] (26 mg, 0.058 mmol) in MeCN (20 mL) was treated over the course of 2 h dropwise with a MeCN solution (10 mL) of $BAr^F{}^*{}_3$ (50 mg, 0.052 mmol). The solvent was then removed under vacuum and the residue was extracted into 5 mL of Et_2O. The extract was passed through Celite and then evaporated under vacuum to yield a tacky red solid, which was triturated with pentane (3 × 10 mL). Yield: 50 mg (68%). Anal. Calcd for $C_{45}BFe_2S_2H_6O_4N_2F_{27}K_2{\cdot}0.33CH_3CN{\cdot}OEt_2$ (found): C, 39.66 (40.03); H, 1.14 (0.88); N, 2.17 (2.03). IR (MeCN): 2096, 2081, 1990, 1978, 1942, 1931, 1913, 1888. IR (CH_2Cl_2): 2100, 1990, 1927.

*$K_2[Fe_2(pdt)(CO)_4(CNBAr^F{}^*{}_3)_2]$, K_2[**1**$(BAr^F{}^*{}_3)_2$].* A solution of K_2[**1**] (24 mg, 0.052 mmol) in MeCN (5 mL) was treated with a solution of $BAr^F{}^*{}_3$ (100 mg, 0.11 mmol) in MeCN (10 mL). The solvent was then removed under vacuum. The residue was extracted into 5 mL of Et_2O, and this extract was treated with 20 mL of pentane, precipitating a red oil that was triturated with pentane (3 × 10 mL) to yield a red solid. Yield: 84 mg (68%). IR (MeCN) 2098, 1991, 1959, 1947, 1932, 1909. IR (CH_2Cl_2): 2119, 1989, 1951, 1916.

*$Et_4N[(\mu\text{-}H)Fe_2(pdt)(CO)_4(CNBAr^F{}_3)_2]$, Et_4N[**H1**$(BAr^F{}_3)_2$].* A solution of $(Et_4N)_2$[**1**$(BAr^F{}_3)_2$] (0.282 g, 0.169 mmol) in ether (50 mL) was treated with HCl in ether (0.093 mL, 2 M, 0.186 mmol). The reaction solution color became lighter, and a colorless precipitate formed. The reaction solution was stirred for 30 min and was filtered through a plug of Celite to remove Et_4NCl. The filtrate was collected, the solvent was evaporated to ca. 10 mL, and pentane (20 mL) was added. The resulting red solid was extracted into ether (10 mL), and this extract was layered with pentane (30 mL) to yield yellow microcrystals. Yield: 107 mg (44%). Anal. Calcd for $C_{53}B_2Fe_2S_2H_{27}O_4N_3F_{30}$ (found): C, 41.41 (41.29); H, 1.77 (1.75); N, 2.73 (2.66). IR (CH_2Cl_2): 2185, 2071, 2051, 2022. ^1H NMR (CD_2Cl_2): δ −13.7 (s, Fe-*H*), −16.4 (s, Fe-*H*), −19.0 (s, Fe-*H*). ^{19}F NMR (CD_2Cl_2): δ −134.8 (dd, *o*-F), −134.9 (m, *o*-F), −160.4 (t, *p*-F), −160.8 (t, *p*-F), −160.9 (t, *p*-F), −166.2 (m, *m*-F), −166.5 (td, *m*-F), −166.6 (td, *m*-F). ^{11}B NMR (CD_2Cl_2): δ −15.

*$Et_4N[(\mu\text{-}H)Fe_2(pdt)(CO)_4(CNBAr^{F\#}{}_3)_2]$, Et_4N[**H1**$(BAr^{F\#}{}_3)_2$].* A solution of $(Et_4N)_2$[**1**$(BAr^{F\#}{}_3)_2$] (100 mg, 0.069 mmol) in THF (1 mL) was treated with a solution of HCl in ether (0.1 mL, 2M, 0.2 mmol), resulting in the color of the solution lightening and the appearance of some solid precipitate. The reaction solution was cooled to −30 °C to precipitate Et_4NCl and was then filtered through a plug of Celite. The solution was evaporated under vacuum, and the resulting oil was triturated with pentane (3 × 10 mL) and left to dry under vacuum overnight, yielding a red solid. Yield: 91 mg (99%). Anal. Calcd for $C_{53}H_{39}B_2F_{18}Fe_2N_3O_4S_2$ (found): C, 48.18 (48.51); H, 2.97 (3.17); N, 3.18 (3.16). IR (CH_2Cl_2): 2194, 2066, 2046, 2012. ^1H NMR (CD_2Cl_2): δ −16.41 (s, Fe-*H*), −19.16 (s, Fe-*H*). ^{19}F NMR (CD_2Cl_2): δ −100.6 (s, *o*-F), −100.8 (s, *o*-F), −116.1 (s, *p*-F), −116.3 (s, *p*-F).

pK_a Determinations. Solutions of $(Et_4N)_2$[**1**$(BAr^F{}_3)_2$] and $Ph_3NHBAr^{F24}{\cdot}2Et_2O$ or $(Et_4N)_2$[**1**$(BAr^{F\#}{}_3)_2$] and $PyHBAr^{F24}$ were prepared in MeCN with approximate $[\mathbf{1}(BAr_3)_2]^{2-}$/acid ratios of 1:2, 1:1, and 2:1 and examined by ^{19}F NMR spectroscopy. Solutions reached equilibrium at room temperature over 24 h. The pK_a was then determined using the Henderson−Hasselbach equation.

■ ASSOCIATED CONTENT

Ⓢ Supporting Information

Synthetic procedures, IR and NMR spectra, cyclic voltammograms, and .cif files. This material is available free of charge via the Internet at http://pubs.acs.org.

■ AUTHOR INFORMATION

Corresponding Author

*E-mail: rauchfuz@uiuc.edu.

Notes

The authors declare no competing financial interest.

■ ACKNOWLEDGMENTS

This research was supported by the U.S. National Institutes of Health and the International Institute for Carbon Neutral Energy Research (WPI-I2CNER), sponsored by the World

Premier International Research Center Initiative (WPI), MEXT, Japan. We thank Dr. D. Gray for assistance with the crystallography.

REFERENCES

(1) (a) Pierik, A. J.; Hulstein, M.; Hagen, W. R.; Albracht, S. P. J. *Eur. J. Biochem.* **1998**, *258*, 572. (b) Pierik, A. J.; Roseboom, W.; Happe, R. P.; Bagley, K. A.; Albracht, S. P. J. *J. Biol. Chem.* **1999**, *274*, 3331.
(2) Tard, C.; Pickett, C. J. *Chem. Rev.* **2009**, *109*, 2245.
(3) Knorzer, P.; Silakov, A.; Foster, C. E.; Armstrong, F. A.; Lubitz, W.; Happe, T. *J. Biol. Chem.* **2012**, *287*, 1489.
(4) Ogata, H.; Lubitz, W.; Higuchi, Y. *Dalton Trans.* **2009**, 7577.
(5) Mulder, D. W.; Ratzloff, M. W.; Shepard, E. M.; Byer, A. S.; Noone, S. M.; Peters, J. W.; Broderick, J. B.; King, P. W. *J. Am. Chem. Soc.* **2013**, *135*, 6921.
(6) Schmidt, M.; Contakes, S. M.; Rauchfuss, T. B. *J. Am. Chem. Soc.* **1999**, *121*, 9736.
(7) Lyon, E. J.; Georgakaki, I. P.; Reibenspies, J. H.; Darensbourg, M. Y. *Angew. Chem., Int. Ed.* **1999**, *38*, 3178. Le Cloirec, A.; Best, S. P.; Borg, S.; Davies, S. C.; Evans, D. J.; Hughes, D. L.; Pickett, C. J. *Chem. Commun.* **1999**, 2285.
(8) Jablonskytė, A.; Wright, J. A.; Pickett, C. J. *Dalton Trans.* **2010**, *39*, 3026.
(9) Zhao, X.; Georgakaki, I. P.; Miller, M. L.; Yarbrough, J. C.; Darensbourg, M. Y. *J. Am. Chem. Soc.* **2001**, *123*, 9710.
(10) Gloaguen, F.; Lawrence, J. D.; Schmidt, M.; Wilson, S. R.; Rauchfuss, T. B. *J. Am. Chem. Soc.* **2001**, *123*, 12518.
(11) Camara, J. M.; Rauchfuss, T. B. *Nat. Chem.* **2012**, *4*, 26. Zaffaroni, R.; Rauchfuss, T. B.; Gray, D. L.; De Gioia, L.; Zampella, G. *J. Am. Chem. Soc.* **2012**, *134*, 19260.
(12) Carroll, M. E.; Barton, B. E.; Rauchfuss, T. B.; Carroll, P. J. *J. Am. Chem. Soc.* **2012**, *134*, 18843.
(13) Pandey, A. S.; Harris, T. V.; Giles, L. J.; Peters, J. W.; Szilagyi, R. K. *J. Am. Chem. Soc.* **2008**, *130*, 4533.
(14) Greco, C.; Bruschi, M.; Heimdal, J.; Fantucci, P.; De Gioia, L.; Ryde, U. *Inorg. Chem.* **2007**, *46*, 7256.
(15) Fourmond, V.; Greco, C.; Sybirna, K.; Baffert, C.; Wang, P.-H.; Ezanno, P.; Montefiori, M.; Bruschi, M.; Meynial-Salles, I.; Soucaille, P.; Blumberger, J.; Bottin, H.; De Gioia, L.; Léger, C. *Nat. Chem.* **2014**, *6*, 336.
(16) Rocchini, E.; Rigo, P.; Mezzetti, A.; Stephan, T.; Morris, R. H.; Lough, A. J.; Forde, C. E.; Fong, T. P.; Drouin, S. D. *J. Chem. Soc., Dalton Trans.* **2000**, 3591. Zhou, J. M.; Lancaster, S. J.; Walker, D. A.; Beck, S.; Thornton-Pett, M.; Bochmann, M. *J. Am. Chem. Soc.* **2001**, *123*, 223.
(17) Brunkan, N. M.; Brestensky, D. M.; Jones, W. D. *J. Am. Chem. Soc.* **2004**, *126*, 3627.
(18) Vei, I. C.; Pascu, S. I.; Green, M. L. H.; Green, J. C.; Schilling, R. E.; Anderson, G. D. W.; Rees, L. H. *Dalton Trans.* **2003**, 2550.
(19) Stephan, D. W.; Erker, G. *Angew. Chem., Int. Ed.* **2010**, *49*, 46.
(20) Luo, L.; Marks, T. J. *Top. Catal.* **1999**, *7*, 97.
(21) (a) Erker, G. *Dalton Trans.* **2005**, 1883. (b) Piers, W. E. *Adv. Organomet. Chem.* **2005**, *52*, 1.
(22) Britovsek, G. J. P.; Ugolotti, J.; White, A. J. P. *Organometallics* **2005**, *24*, 1685.
(23) Manor, B. C.; Rauchfuss, T. B. *J. Am. Chem. Soc.* **2013**, *135*, 11895.
(24) Lawrence, J. D.; Li, H. X.; Rauchfuss, T. B.; Benard, M.; Rohmer, M. M. *Angew. Chem., Int. Ed.* **2001**, *40*, 1768.
(25) (a) Coffey, C. E. *J. Inorg. Nucl. Chem.* **1963**, *25*, 179. (b) Darensbourg, D. J.; Reibenspies, J. H.; Lai, C. H.; Lee, W. Z.; Darensbourg, M. Y. *J. Am. Chem. Soc.* **1997**, *119*, 7903.
(26) Boyer, J. L.; Rauchfuss, T. B.; Wilson, S. R. *C. R. Chim.* **2008**, *11*, 922.
(27) (a) Morrison, D. J.; Piers, W. E. *Org. Lett.* **2003**, *5*, 2857. (b) Welch, G. C.; Cabrera, L.; Chase, P. A.; Hollink, E.; Masuda, J. D.; Wei, P. R.; Stephan, D. W. *Dalton Trans.* **2007**, 3407.
(28) Nicasio, J. A.; Steinberg, S.; Ines, B.; Alcarazo, M. *Chem.—Eur. J.* **2013**, *19*, 11016.
(29) Durfey, B. L.; Gilbert, T. M. *Inorg. Chem.* **2011**, *50*, 7871.
(30) Chakraborty, D.; Rodriguez, A.; Chen, E. Y. X. *Macromolecules* **2003**, *36*, 5470.
(31) Zhao, X.; Georgakaki, I. P.; Miller, M. L.; Mejia-Rodriguez, R.; Chiang, C. Y.; Darensbourg, M. Y. *Inorg. Chem.* **2002**, *41*, 3917.
(32) Nehring, J. L.; Heinekey, D. M. *Inorg. Chem.* **2003**, *42*, 4288.
(33) Kaljurand, I.; Kutt, A.; Soovali, L.; Rodima, T.; Maemets, V.; Leito, I.; Koppel, I. A. *J. Org. Chem.* **2005**, *70*, 1019.
(34) Boyke, C. A. PhD Thesis, University of Illinois at Urbana-Champaign, 2006.
(35) Bradley, D. C.; Harding, I. S.; Keefe, A. D.; Motevalli, M.; Zheng, D. H. *J. Chem. Soc., Dalton Trans.* **1996**, 3931.
(36) Besora, M.; Lledos, A.; Maseras, F. *Chem. Soc. Rev.* **2009**, *38*, 957.
(37) Wang, N.; Wang, M.; Zhang, T. T.; Li, P.; Liu, J. H.; Sun, L. C. *Chem. Commun.* **2008**, 5800.
(38) Eilers, G.; Schwartz, L.; Stein, M.; Zampella, G.; de Gioia, L.; Ott, S.; Lomoth, R. *Chem.—Eur. J.* **2007**, *13*, 7075.
(39) Jablonskytė, A.; Wright, J. A.; Fairhurst, S. A.; Peck, J. N. T.; Ibrahim, S. K.; Oganesyan, V. S.; Pickett, C. J. *J. Am. Chem. Soc.* **2011**, *133*, 18606.
(40) Berggren, G.; Adamska, A.; Lambertz, C.; Simmons, T. R.; Esselborn, J.; Atta, M.; Gambarelli, S.; Mouesca, J. M.; Reijerse, E.; Lubitz, W.; Happe, T.; Artero, V.; Fontecave, M. *Nature* **2013**, *499*, 66.
(41) Greco, C.; Bruschi, M.; Fantucci, P.; Ryde, U.; De Gioia, L. *Chem.—Eur. J.* **2011**, *17*, 1954.
(42) Mack, A. E.; Rauchfuss, T. B.; Ohnishi, K.; Ohki, Y.; Tatsumi, K. *Inorg. Synth.* **2010**, *35*, 143.
(43) Reynard, K. E.; Sherman, R. E.; Smith, H. D.; Hohnstedt, L. F.; Gassenheimer, G.; Wartik, T. *Inorg. Synth.* **2007**, 52.
(44) Travis, A. L.; Binding, S. C.; Zaher, H.; Arnold, T. A. Q.; Buffet, J. C.; O'Hare, D. *Dalton Trans.* **2013**, *42*, 2431.